THE JOURNAL OF BIOLOGICAL CHEMISTRY VOL. 288, NO. 19, pp. 13831–13841, May 10, 2013

Enhanced Asynchronous Ca^{2+} Oscillations Associated with Impaired Glutamate Transport in Cortical Astrocytes Expressing *Fmr1* Gene Premutation Expansion*

Received for publication, December 1, 2012, and in revised form, April 2, 2013 Published, JBC Papers in Press, April 3, 2013, DOI 10.1074/jbc.M112.441055

Zhengyu Cao[‡1], Susan Hulsizer[‡], Yanjun Cui[‡], Dalyir L. Pretto[§], Kyung Ho Kim[‡2], Paul J. Hagerman[§¶], Flora Tassone[§¶], and Isaac N. Pessah[‡¶]

From the [‡]Department of Molecular Biosciences, School of Veterinary Medicine, [§]Department of Biochemistry and Molecular Medicine, School of Medicine, and [¶]Medical Investigations of Neurodevelopmental Disorders (MIND) Institute, University of California, Davis, California 95616

Background: *FMR1* CGG expansion repeats in the premutation range have not been linked to astrocyte pathophysiology.
Results: Premutation cortical astrocytes display decreased Glu transporter expression/activity and enhanced asynchronous Ca^{2+} oscillations.
Conclusion: Glu transport and Ca^{2+} signaling defects in premutation astrocytes could contribute to FXTAS neuropathology.
Significance: Premutation astrocytes may have an etiological role in FXTAS neuropathology.

Premutation CGG repeat expansions (55–200 CGG repeats; preCGG) within the fragile X mental retardation 1 (*FMR1*) gene can cause fragile X-associated tremor/ataxia syndrome. Defects in early neuronal migration and morphology, electrophysiological activity, and mitochondria trafficking have been described in a premutation mouse model, but whether preCGG mutations also affect astrocyte function remains unknown. PreCGG cortical astrocytes (~170 CGG repeats) displayed 3-fold higher *Fmr1* mRNA and 30% lower *FMR1* protein (FMRP) when compared with WT. PreCGG astrocytes showed modest reductions in expression of glutamate (Glu) transporters GLT-1 and GLAST and attenuated Glu uptake ($p < 0.01$). Consistent with astrocyte cultures *in vitro*, aged preCGG mice cerebral cortex also displayed reduced GLAST and GLT-1 expression. Approximately 65% of the WT and preCGG cortical astrocytes displayed spontaneous asynchronous Ca^{2+} oscillations. PreCGG astrocytes exhibited nearly 50% higher frequency of asynchronous Ca^{2+} oscillations ($p < 0.01$) than WT, a difference mimicked by chronic exposure of WT astrocytes to L-*trans*-pyrrolidine-2,4-dicarboxylic acid (L-*trans*-PDC) or by partial suppression of GLAST using siRNA interference. Acute challenge with Glu augmented the frequency of Ca^{2+} oscillations in both genotypes. Additionally, 10 μM Glu elicited a sustained intracellular Ca^{2+} rise in a higher portion of preCGG astrocytes when compared with WT. Pharmacological studies showed that mGluR5, but not NMDA receptor, contributed to Glu hypersensitivity in preCGG astrocytes. These functional defects in preCGG astrocytes, especially in Glu signaling, may contribute to fragile X-associated tremor/ataxia syndrome neuropathology.

Fragile X-associated tremor/ataxia syndrome (FXTAS)[3] is a late adult onset neurodegenerative disorder that occurs in individuals with a trinucleotide expansion (55–200 CGG repeats, premutation) within the fragile-X mental retardation 1 (*FMR1*) gene. Premutation alleles of the *FMR1* gene have estimated frequencies of 1:130–250 females and 1:250–810 males (1, 2). These premutation carriers can display clinical features including behavioral and cognitive abnormalities in children (3–6), primary ovarian insufficiency in ~20% of women (7), and FXTAS (7–9) in ~40% of male carriers. The core clinical features of FXTAS include progressive gait ataxia and intention tremor, dysautonomia, peripheral neuropathy, and parkinsonism (7, 8, 10, 11). Larger CGG expansions (>200 repeats; full mutation) generally result in hypermethylation of the *FMR1* gene with subsequent transcriptional silencing. The absence of the *FMR1* protein (FMRP) leads to fragile X syndrome (FXS), the most common inherited form of cognitive impairment and a leading single-gene disorder associated with autism (12, 13). Consistent with observations in human premutation carriers (14), premutation CGG expansion (preCGG) mouse neurons display elevated *Fmr1* mRNA and normal to variable reductions on the FMRP in brain lysate (15, 16). The absence of fragile X-associated primary ovarian insufficiency and FXTAS symptoms in full mutation patients (FXS) implies that FMRP deficiency *per se* is not responsible for premutation disorders and FXTAS. Excessive *FMR1* mRNA is hypothesized to be toxic to neurons and glia (1, 17–20). However, whether the partial

* This work was supported, in whole or in part, by National Institutes of Health Grants RC1 AG036022 (to P. J. H. and I. N. P.), 1R01 HD064817 (to I. N. P.), and P01ES011269 (to I. N. P.). This work was also supported by the United States Environmental Protection Agency Grants R833292 and R829388 (to I. N. P.) and HD02274 (to F. T.).

[1] To whom correspondence should be addressed: Molecular Biosciences, University of California Davis, 1 Shields Ave., Davis, CA 95616. Tel.: 530-752-2174; Fax: 530-752-4698; E-mail: zcao@ucdavis.edu.

[2] Present address: Dept. of Biochemistry and Biomedical Sciences, College of Medicine, Seoul National University, 103 Daehak-ro, Jongno-gu, Seoul 110-799, Korea.

[3] The abbreviations used are: FXTAS, fragile X-associated tremor/ataxia syndrome; FMRP, *FMR1* protein; FXS, fragile X syndrome; preCGG, premutation CGG expansion; L-*trans*-PDC, L-*trans*-pyrrolidine-2,4-dicarboxylic acid; GLAST, glutamate aspartate transporter; GFAP, glial fibrillary acidic protein; EAAT, excitatory amino acid transporter; MPEP, 2-methyl-6-(phenylethynyl)pyridine; DHPG, dihydroxyphenylglycine; mGluR, metabotropic glutamate receptor; KI, knock-in; P, postnatal day; CI, confidence intervals.

loss of FMRP in premutation carriers also contributes to the onset or progression of premutation disorders and FXTAS is not well established. Defects in neuronal morphology (21) and migration (22), aberrant spontaneous Ca^{2+} oscillations and clustered bursts of electrical firing (23), as well as abnormalities in the number, mobility, and metabolic function of mitochondria in the early stages of neuron differentiation in preCGG mouse model (24) have been reported.

Astrocytes actively modulate synaptic activity and synaptic network by releasing gliotransmitters such as glutamate (Glu), ATP, and D-serine in a Ca^{2+}-dependent manner (25, 26). Defects in astrocytes and their impact on neuronal cell development have been reported in FXS (27, 28) and other neurodevelopmental disorders such as Rett syndrome (29–31). Normal astrocytes can prevent aberrant neuronal development in the *Fmr1* knock-out (KO) mouse; conversely, fragile X astrocytes are capable of inducing developmental delays in dendrite maturation and synaptic protein expression (27, 28). Premutation mouse astrocytes display ubiquitin-positive intranuclear inclusions (15, 32), which are the neuropathological hallmark of FXTAS (19, 33). Moreover, the ubiquitin-positive intranuclear inclusions are present notably in a higher percentage in human cortical gray matter astrocytes (17%) than in neurons (4%) (18, 19, 33). These data indicate that the *FMR1* CGG expansion repeats in the premutation range might also trigger functional abnormalities in astrocytes that promote neuropathology. However, little is known about astrocyte defects related to the presence of premutation CGG expansions.

Here, we report that cortical astrocytes cultured from hemizygous male pups with the *Fmr1* allele expanded in the high premutation range (~170 CGG repeats, designated preCGG throughout) display elevated *Fmr1* mRNA and a moderate decrease of FMRP. When compared with the wild type (WT) controls, preCGG cortical astrocytes exhibit more frequent spontaneous Ca^{2+} oscillations and reduced expression of Glu transporters GLAST and GLT-1, consistent with attenuated Glu uptake. Pharmacological suppression of Glu transporters activity or decrease in the GLAST expression using GLAST siRNA enhances spontaneous asynchronous Ca^{2+} oscillations in WT astrocytes similar to those observed in preCGG astrocytes, suggesting that reduced Glu uptake may contribute to altered Ca^{2+} dynamics observed in preCGG astrocytes.

EXPERIMENTAL PROCEDURES

Antibodies and siRNA—GLAST antibody was purchased from Santa Cruz Biotechnology, Inc. (Santa Cruz, CA). GLT-1 antibody was from Alpha Diagnostic International (San Antonio, TX). Anti-mGluR1/5 antibody was from University of California Davis/National Institutes of Health NeuroMab Facility (Davis, CA). FMRP antibody was produced as described previously (34). Predesigned GLAST siRNA pool (catalog number L-056182-01-0005) or nontargeting siRNA (catalog number D-001810-01-05) was from Thermo Scientific.

Animals and Genotyping—All preCGG KI and WT mice in the C57/B6 background were housed under standard vivarium conditions. PreCGG hemizygous male pups (range 155–200; average 170 CGG repeats) were obtained by breeding homozygous preCGG females with preCGG hemizygous males. Male WT pups delivered on the same day as male preCGG pups were used for paired cultures. The University of California, Davis Institutional Animal Care and Use Committee (IACUC) approved all animal use protocols. Genotypes were verified by PCR for each individual pup using *Fmr1* forward and reverse specific primers as described previously (23).

Cortical Astrocyte Cultures and Transfection—Cortical astrocytes were obtained from postnatal day 0–1 (P0–1) WT or hemizygous preCGG KI male pups. The dissection and dissociation of cortical cells were performed as described previously (35). The dissociated cells were plated onto a poly-L-ornithine-coated T-75 culture flask at a density of $1.0–1.5 \times 10^7$ cells/flask and maintained in culture medium (DMEM + 10% FBS) in an incubator at 37 °C with 5% CO_2 and 95% humidity. The culture medium was changed twice a week, and the cells were used between 2 and 4 weeks with no more than three passages. WT astrocytes were transfected with predesigned GLAST siRNA pool or nontargeting siRNA using DharmaFECT 1 transfection reagent (catalog number T-2001-01, Thermo Scientific) in serum-free culture medium. The final concentration of siRNA was 25 nM. The serum-free medium was replaced with culture medium after 24 h, and the astrocytes were cultured for another 48 h prior to harvest the samples for Western blot analysis.

Quantitative Measurements of Fmr1 mRNA—Total RNA from primary cortical astrocytes from both WT and preCGG KI mice was isolated by standard method (TRIzol, Ambion Inc., Austin, TX). Quantitative measurements of *Fmr1* mRNA levels from total RNA were obtained by real time PCR as described previously (14).

Western Blots—Equal amounts (20 μg) of cell lysates were loaded onto a 10% SDS-PAGE gel and transferred to a nitrocellulose membrane by electroblotting. After blocking with Odyssey blocking buffer (LI-COR Biotechnology, Lincoln, NE), the membranes were incubated with primary antibody overnight at 4 °C or 2 h at room temperature (anti-FMRP, 1:20,000; anti-tubulin, 1:10,000; anti-GLT-1, 1:1,000; anti-GLAST, 1:500; anti-GFAP, 1:10,000; and anti-mGluR1/5, 1:2000). After washing, the IRDye (800CW or 700CW)-labeled secondary antibody (LI-COR Biotechnology, 1:10,000 dilution) was added, and the blots were incubated for 1 h at room temperature. The membrane was imaged with the LI-COR Odyssey infrared imaging system (LI-COR Biotechnology). The densitometry analysis was performed using LI-COR Odyssey infrared imaging system application software 2.1.

Immunocytochemistry—After briefly being washed with PBS twice, astrocytes were fixed with 4% paraformaldehyde for 15 min. Cells were permeabilized with 0.1% Triton X-100 for 20 min. Following blocking with PBS containing 2% glycerol, 0.05 M NH_4Cl, 5% PBS, and 2% goat serum for 2 h, cells were incubated with rabbit anti-GFAP (Dako, Glostrup, Denmark, 1:1,000) overnight at 4 °C. After washing with PBS for 5 min, cells were incubated with Alexa Fluor 568-conjugated goat anti-rabbit secondary antibody (1:500, Molecular Probes, Eugene, OR) for 1 h at room temperature. The cells were then washed and mounted in Prolong Gold antifade mounting medium with DAPI (Molecular Probes) and visualized in an

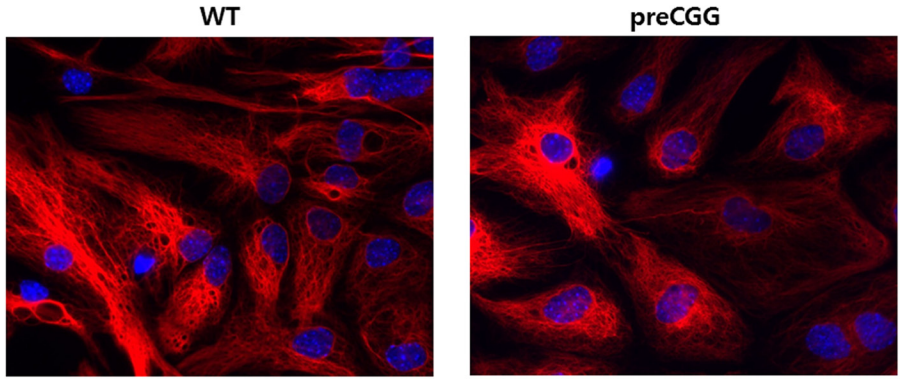

FIGURE 1. **Representative GFAP immunocytochemistry of astrocytes cultured from WT mice and knock-in *FMR1* premutation (preCGG) mice.** WT and preCGG cortical astrocytes exhibit similar morphology when stained with GFAP. Nearly all the cells were GFAP-positive in both WT and preCGG cortical astrocyte culture, indicating a high enrichment of astrocytes in our culture.

IX-71 invert microscope (Olympus America, Center Valley, PA).

Ca^{2+} Imaging—After the medium was aspirated, astrocytes were incubated with dye loading buffer (100 μl/well) containing 4 μM Fluo-4 and 0.5 mg/ml BSA in Locke's buffer (35) for 30 min. The cells were excited at 488 nm using a DeltaRam illuminator (Photon Technologies International, Birmingham, NJ), and fluorescence emission was recorded at 525 nm. The images were captured with an Evolve® cooled charge-coupled device camera (Photometrics, Tucson, AZ) attached to an inverted Olympus IX71 microscope (Olympus America). The Fluo-4 fluorescent arbitrary signals were captured and analyzed for individual cells using EasyRatioPro software (Photon Technologies International, Birmingham, NJ). Data were presented as F/F_0. To measure population responses to Glu challenge, the cells were plated and loaded with Fluo-4 as described above, and changes in intracellular Ca^{2+} concentration was determined as described previously using a fluorescent imaging plate reader (FLIPR® Tetra Station, Molecular Devices, Sunnyvale, CA) (36).

[^{3}H]Glu Uptake Assay—The cortical astrocytes were plated onto poly-L-ornithine-coated 48-well plates at an initial density of 100,000 cells/well and cultured for 24–48 h until 90% confluent. The [^{3}H]Glu (Moravek Biochemicals and Radiochemicals; 27 Ci/mmol) uptake assay was performed at room temperature. The astrocytes were incubated with 100 μM Glu for 30 min in Locke's buffer. After washing with ice-cold PBS, the cells were lysed by the addition of 300 μl of 0.5% SDS solution, and the lysates were subjected to liquid scintillation counting for determining the radioactivity. For each genotype, three adjacent wells were used to determine the protein concentration using the BCA method, and Glu uptake values were adjusted to protein content.

Data Analysis—Graphing and statistical analyses were performed using GraphPad Prism software (GraphPad Software Inc., San Diego, CA). Statistical significance between WT and preCGG was calculated using Student's t test, and p values below 0.05% were considered significant. The EC_{50} values and maximal response for Glu response were determined by nonlinear regression analysis using a logistic equation. Kinetic parameters (K_m and V_{max}) for Glu uptake were determined by nonlinear regression analysis of the saturation curves using the Michaelis-Menten equation.

RESULTS

PreCGG Cortical Astrocytes Display Elevated Fmr1 mRNA and Modestly Reduced FMRP—Given the ubiquitin-positive nuclear inclusions observed in astrocytes in the brains of preCGG KI mice (15, 32), we first examined the *Fmr1* mRNA levels in both preCGG and WT cortical astrocyte cultures. The purity of cultured astrocytes was evaluated by labeling the cells with DAPI and the astrocyte-specific markers, glial fibrillary acidic protein (GFAP). As shown in Fig. 1, greater than 95% of the cells used in these experiments were GFAP-positive, indicating enrichment of astrocytes in our cultures. The *Fmr1* levels in the cortical astrocytes cultured from the preCGG mice were 311 ± 50% ($n = 6$, $p < 0.01$) of WT control (Fig. 2*a*). Western blot analysis was used to measure FMRP expression using β-tubulin as a control for the protein loading. PreCGG cortical astrocytes displayed 70.1 ± 7.2% ($n = 4$, $p < 0.01$) of WT control on the FMRP expression (Fig. 2, *b* and *c*).

PreCGG Cortical Astrocytes Display Enhanced Spontaneous Asynchronous Ca^{2+} Oscillations—WT and preCGG astrocytes exhibited similar morphology when stained with GFAP (Fig. 1). When loaded with the Ca^{2+} indicator Fluo-4 and monitored by fluorescence imaging, astrocytes display spontaneous asynchronous Ca^{2+} oscillations previously shown to correlate with the release of gliotransmitters that regulate local neuronal cell networks (38). We examined the Ca^{2+} dynamics in WT and preCGG cortical astrocytes cultured on the same day. Consistent with previous studies, WT cortical astrocyte cultures display asynchronous Ca^{2+} oscillations (Fig. 3*a*) that are distinctly different from the synchronous Ca^{2+} oscillation observed in cortical neurons, which oscillate at much higher frequencies and shorter durations (35). The distinct temporal characteristics of asynchronous Ca^{2+} oscillations ensure that the signals recorded and analyzed were from astrocytes, not neurons in our culture system. The percentage of astrocytes that were oscillatory did not differ significantly between WT (65.3 ± 3.3%, n = 20 wells) and preCGG (70.6 ± 3.0%, n = 16 wells) (Fig. 3*c*). However, the preCGG astrocytes displayed more spontaneous Ca^{2+} oscillations when compared with WT control (Fig. 3*d*). Of

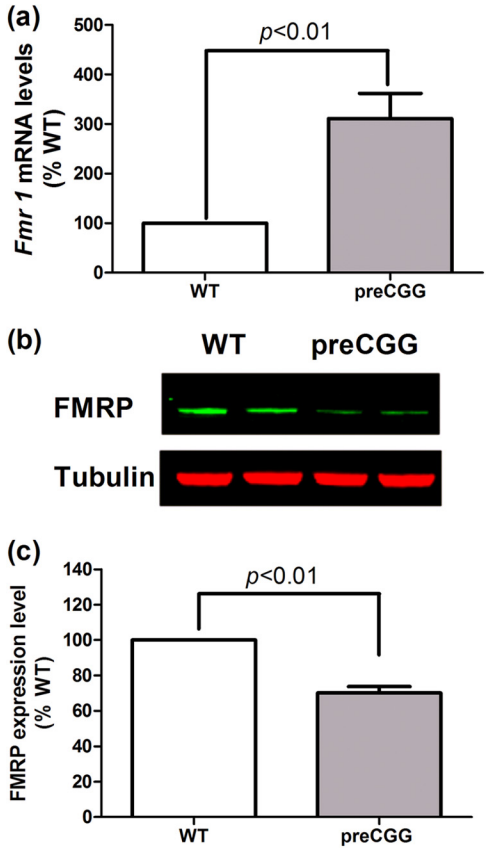

FIGURE 2. **PreCGG cortical astrocytes display higher *Fmr1* mRNA level and reduced FMRP proteins when compared with WT controls.** *a*, *Fmr1* mRNA level comparison between WT and preCGG astrocytes. Quantitative RT-PCR was performed, and *Fmr1* mRNA level was measured. PreCGG astrocytes showed 311 ± 50% (mean ± S.E.) of the WT control ($p < 0.01$, $n = 6$). *b*, representative Western blotting for FMRP expression in WT and preCGG cortical astrocytes. *c*, quantification of FMRP expression in WT and preCGG cortical cultures. PreCGG cortical astrocytes displayed 70.1 ± 7.2% of WT control ($p < 0.01$, $n = 4$).

the cells that were oscillatory, the average frequency of spontaneous Ca^{2+} oscillations for preCGG astrocyte was 4.68 ± 0.21/10 min ($n = 431$ cells), representing 148.6 ± 6.6% ($p < 0.01$) of the WT control (3.15 ± 0.14/10 min, $n = 450$ cells).

PreCGG Cortical Astrocytes and Brain Cortex Display Modest Decrease in the Expression of GLT-1 and GLAST—Glu is the most abundant excitatory neurotransmitter in the vertebrate CNS. The excitatory amino acid transporters (EAATs) are responsible for the rapid removal of Glu from the extracellular space and maintain Glu concentration at a subtoxic level. Within the EAATs family, Glu transporters GLAST (EAAT1 in human) and GLT-1 (EAAT2 in human) are highly expressed in glial cells, where they are the primary Glu uptake mechanism in the mammalian central nervous system (39). We examined the expression of GLT-1 and GLAST using Western blot analysis. As shown in Fig. 4, the expression levels for GLAST and GLT-1 in preCGG cortical astrocytes were slightly, although significantly decreased, representing 88.6 ± 2.4% ($p < 0.05$, $n = 4$) and 92.1 ± 1.8% ($p < 0.01$, $n = 6$) of WT controls, respectively. To test whether reduced expression of the major Glu transporters extends to the brain of aging (46–59-week-old) preCGG mutation mice, cortical tissue was dissected, and protein was extracted in lysis buffer. These aged mice used were 50 ± 3 weeks (WT, $n = 4$) and 53 ± 1.3 weeks (preCGG, $n = 4$). As shown in Fig. 5, the expression of GLAST was significantly decreased to 72.3 ± 3.1% ($p < 0.01$, $n = 4$) of WT control. The averaged expression of GLT-1 was 77.2 ± 17.8% of WT control (three out of four mice displayed decreased GLT-1 expression with one mouse having slightly increased GLT-1 expression level). However, due to the variation in the preCGG group, the decrease of GLT-1 expression could not reach statistical significance.

PreCGG Cortical Astrocytes Display Reduced Glu Uptake—We next evaluated the Glu uptake kinetics in both WT and preCGG cortical astrocyte cultures. The astrocytes were incubated with 100 μM Glu (a combination of [^{3}H]Glu (50 nM) and unlabeled Glu) for 30 min in Locke's buffer. The Glu uptake was 99.1 ± 2.0 and 96.9 ± 1.4 nmol/mg of protein over 30 min in WT and preCGG cortical astrocytes, respectively (data not shown). To confirm that Glu transporters mediated Glu uptake, a nonselective Glu transporter inhibitor L-*trans*-PDC was applied 25 min prior to incubating the cells with Glu. L-*trans*-PDC (1 mM) completely inhibited Glu uptake in both WT and preCGG cortical astrocytes (data not shown). We then analyzed the kinetics of the Glu uptake by WT and preCGG cortical astrocytes. Preliminary data demonstrated that with a Glu concentration of 100 μM, the uptake rate was linear for at least 10 min with an r^2 of 0.9799 (data not shown), and therefore, kinetic analyses were performed within 10 min. Uptake as a function of Glu concentration was fitted by the Michaelis-Menten equation. The half-maximal transport constant (K_m) was similar between WT (33.38 (29.79–36.96) μM, mean and 95% confidence intervals (95% CI)), and preCGG astrocytes (31.39 (27.82–34.95) μM, mean and 95% CI). However, preCGG cortical astrocytes displayed reduced maximal Glu uptake rate (V_{max}) (4.79 (4.62–4.97) nmol/mg of protein/min, mean and 95% CI) when compared with the WT controls (5.29 (5.10–5.47) nmol/mg of protein/min, mean and 95% CI) (Fig. 6). This modest yet statistically significant decrease on the V_{max} in preCGG cortical astrocytes is consistent with decreased expression levels of Glu transporters.

L-trans-PDC Enhances Ca^{2+} Oscillation Frequency in WT Cortical Astrocytes—To examine the potential role for Glu transporters on the modulation of spontaneous Ca^{2+} oscillations, we pharmacologically suppressed Glu transporter activity by chronic exposure (48 h) of WT cortical astrocytes to low concentrations (1 and 10 μM) of L-*trans*-PDC. Based on the K_i value of L-*trans*-PDC (40), 10 μM L-*trans*-PDC would be predicted to inhibit 10–15% of the Glu transporters. Therefore, a concentration of 10 μM L-*trans*-PDC may mimic the cellular effect observed in the preCGG cortical astrocytes that displayed modest decrease (~10%) in Glu uptake. As shown in Fig. 7, exposure of WT cortical astrocytes to 10 μM L-*trans*-PDC produced a statistically significant enhancement on the Ca^{2+} oscillations (139.1 ± 9.4%; $p < 0.01$, $n = 94$ cells) when compared with vehicle-treated WT astrocytes, which was comparable with that observed in preCGG cortical astrocytes. Cells exposed to the lower concentration of L-*trans*-PDC (1 μM) elicited a slight although statistically nonsignificant increase in the frequency of Ca^{2+} oscillations (109.1 ± 7.4% of WT, $p > 0.05$, $n = 73$ cells). Together these data demonstrate that suppression of

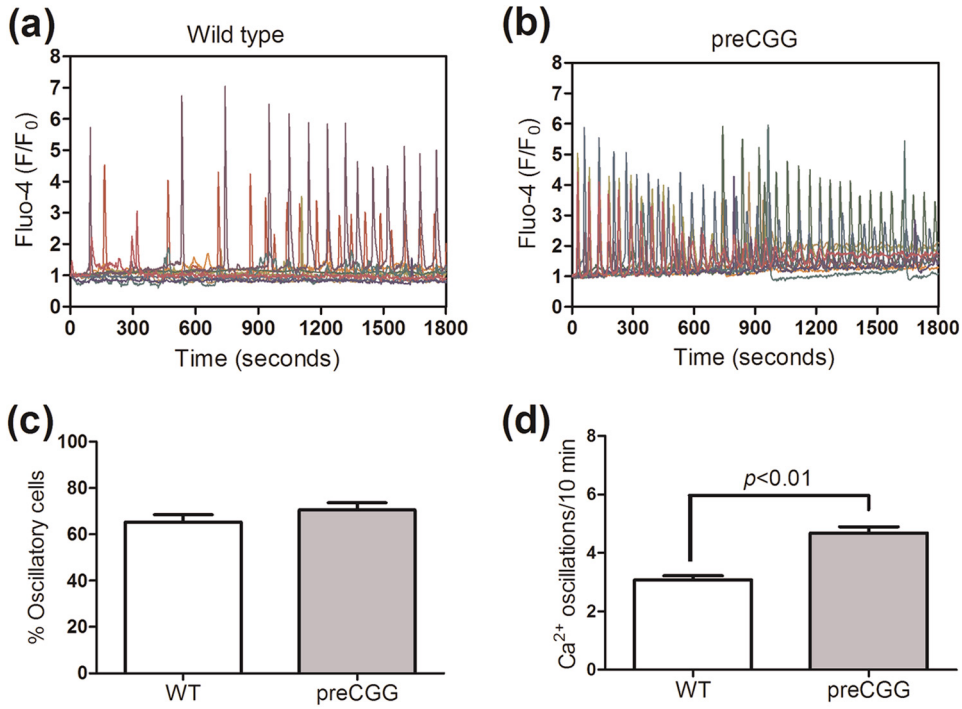

FIGURE 3. **PreCGG mutation mouse cortical astrocytes display more spontaneous Ca^{2+} oscillations.** *a* and *b*, representative ten Ca^{2+} traces in WT (*a*) and preCGG (*b*) cortical astrocytes, respectively. Data are presented as F/F_0. *c*, quantification of the percentage of oscillatory cells in WT and preCGG cortical astrocytes. The percentages of oscillatory astrocytes were 65.3 ± 3.3% ($n = 20$ wells) in preCGG cortical astrocytes and 70.6 ± 3.0% ($n = 16$ wells, $p > 0.05$) in WT controls. *d*, quantification of Ca^{2+} oscillation frequency in WT and preCGG oscillatory cortical astrocytes. PreCGG cortical astrocytes displayed more Ca^{2+} oscillations (4.68 ± 0.21/10 min, $n = 431$ cells) than WT control (3.15 ± 0.14/10 min, $p < 0.01$, $n = 450$ cells).

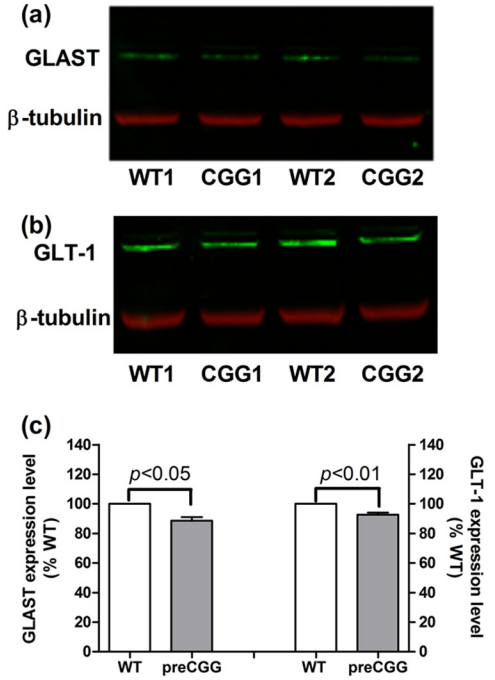

FIGURE 4. **PreCGG cortical astrocytes display lower expression of Glu transporters, GLT-1 and GLAST.** *a* and *b*, representative Western blotting for GLAST (*a*) and GLT-1 (*b*) in WT and preCGG cortical astrocytes. The representative bands were from two independent paired cultures. *c*, quantification of GLAST and GLT-1 expression in WT and preCGG cortical astrocyte cultures, respectively. The expression for GLAST and GLT-1 was 88.6 ± 2.4% ($p < 0.05$, $n = 4$) and 92.1 ± 1.8% ($p < 0.01$, $n = 6$) of WT controls, respectively. These data were from at least three independent paired cultures.

Glu transporter activity can increase the frequency of spontaneous Ca^{2+} oscillations in WT cortical astrocytes that mimics those measured in preCGG, suggesting a potential role for Glu transporter impairment on the modulation of spontaneous Ca^{2+} oscillations in preCGG cortical astrocytes.

Decreased GLAST Expression Level Enhances Ca^{2+} Oscillation Frequency—To further assess the functional significance of Glu transporters on the regulation of spontaneous Ca^{2+} oscillation frequency in astrocytes, we evaluated the spontaneous Ca^{2+} oscillation frequency in the WT astrocytes transfected with GLAST siRNA. Transfection with GLAST siRNA decreased the GLAST expression to 72.1 ± 2.1% ($n = 8$, $p < 0.01$) of the control group (when compared with astrocytes transfected with the nontargeting siRNA) (Fig. 8, *a* and *b*). The astrocytes transfected with GLAST siRNA displayed significantly higher frequency of Ca^{2+} oscillations (3.79 ± 0.20/10 min, $n = 183$) than the astrocytes transfected with nontargeting siRNA (2.25 ± 0.09/10 min, $n = 166$) (Fig. 8*c*).

Glu Augments Spontaneous Ca^{2+} Oscillations in Both Wild Type and preCGG Cortical Astrocytes—An acute challenge with Glu (10 μM) elicited a significant increase on the frequency of spontaneous Ca^{2+} in both WT and preCGG cortical astrocytes (Fig. 9, *a–c*), demonstrating the involvement of Glu receptors on the modulation of spontaneous Ca^{2+} oscillations. In addition to the increase of the frequency on the spontaneous Ca^{2+} oscillations, Glu (10 μM) induced a sustained intracellular Ca^{2+} increase in a fraction of responsive WT and preCGG astrocytes (Fig. 9, *a*, *b*, and *d*). A higher percentage of preCGG astrocytes (23.2 ± 3.7%, $n = 4$ wells) displayed sustained intra-

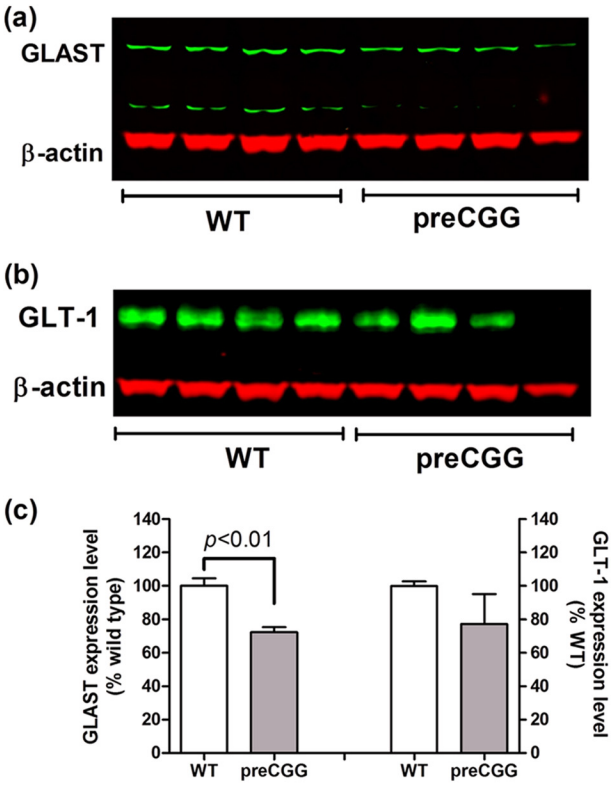

FIGURE 5. **Reduced expression of Glu transporters, GLAST and GLT-1, in preCGG mouse cortex.** *a* and *b*, representative Western blots for GLAST (*a*) and GLT-1 (*b*) in WT and preCGG brain cortex. Each genotype had four mice with an age range of 46–59 weeks ($p > 0.05$). *c*, quantification of GLAST and GLT-1 expression in WT and preCGG mice brain cortex, respectively. The expression for GLAST and GLT-1 was 72.3 ± 3.1% ($p < 0.01$, $n = 4$) and 77.2 ± 17.8% ($p > 0.05$, $n = 4$) of WT controls, respectively.

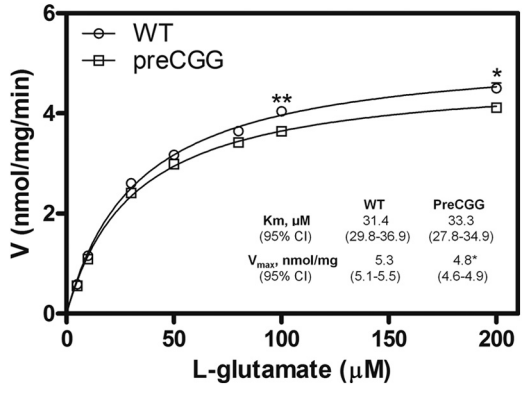

FIGURE 6. **PreCGG astrocytes display decreased Glu uptake.** Kinetic analysis for Glu uptake in WT and preCGG cortical astrocytes was performed. Each data point represents mean ± S.E. ($n = 12$) from four independent cultures performed in triplicates. Uptake as a function of Glu concentration was fitted by the Michaelis-Menten equation. The K_m values for Glu uptake were similar between WT and preCGG cortical astrocytes. However, preCGG cortical astrocytes displayed reduced V_{max} for Glu uptake, which was 5.29 (5.10–5.47 nmol/mg of protein/min, 95% CI) in WT cortical astrocytes and 4.79 (4.62–4.97 nmol/mg of protein/min, 95% CI) in preCGG cortical astrocytes. *, $p < 0.05$, **, $p < 0.01$.

cellular Ca^{2+} increase when compared with WT controls (6.2 ± 1.5%, $n = 11$ wells, $p < 0.01$, Fig. 9*d*). To examine the influence of Glu transporter activity on Glu-induced sustained intracellular Ca^{2+} increase. WT cortical astrocytes were chron-

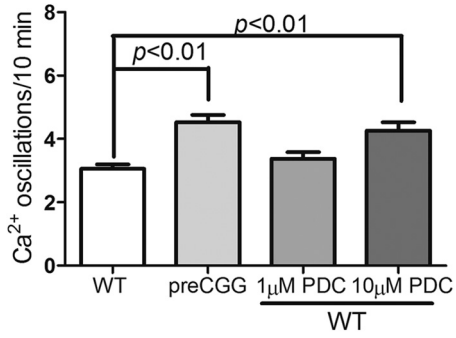

FIGURE 7. **Chronic exposure to low concentrations of L-*trans*-PDC enhances the spontaneous Ca^{2+} oscillations in WT cortical astrocytes.** WT cortical astrocytes chronically exposed to 10 μM L-*trans*-PDC displayed significantly increased Ca^{2+} oscillations when compared with vehicle-treated WT astrocytes. Each data point represents mean ± S.E. with at least 90 cells from two independent cultures.

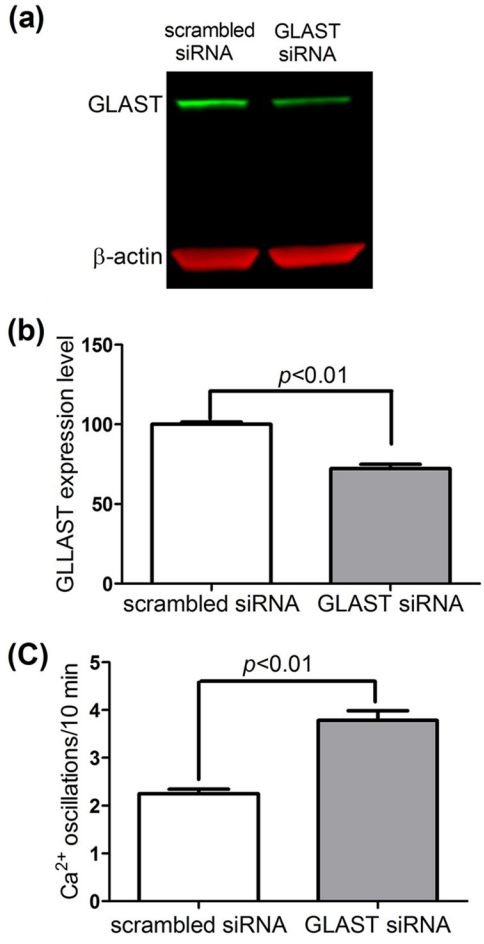

FIGURE 8. **Suppression of GLAST expression enhances the spontaneous Ca^{2+} oscillations in WT cortical astrocytes.** WT cortical astrocytes were transfected with scrambled or GLAST siRNA. *a*, representative Western blot for GLAST expression after transfection with scrambled sequence or GLAST siRNA for 72 h. *b*, quantification of GLAST expression in the astrocytes transfected with scrambled sequence or GLAST siRNA. Transfection with GLAST siRNA decreased GLAST expression to 72.1 ± 2.8% ($n = 8$, $p < 0.01$) of the negative controls. *c*, astrocytes with GLAST siRNA transfection increased asynchronous spontaneous Ca^{2+} oscillations when compared with its negative control. Each data point represents mean ± S.E. with at least 160 cells from four independent cultures.

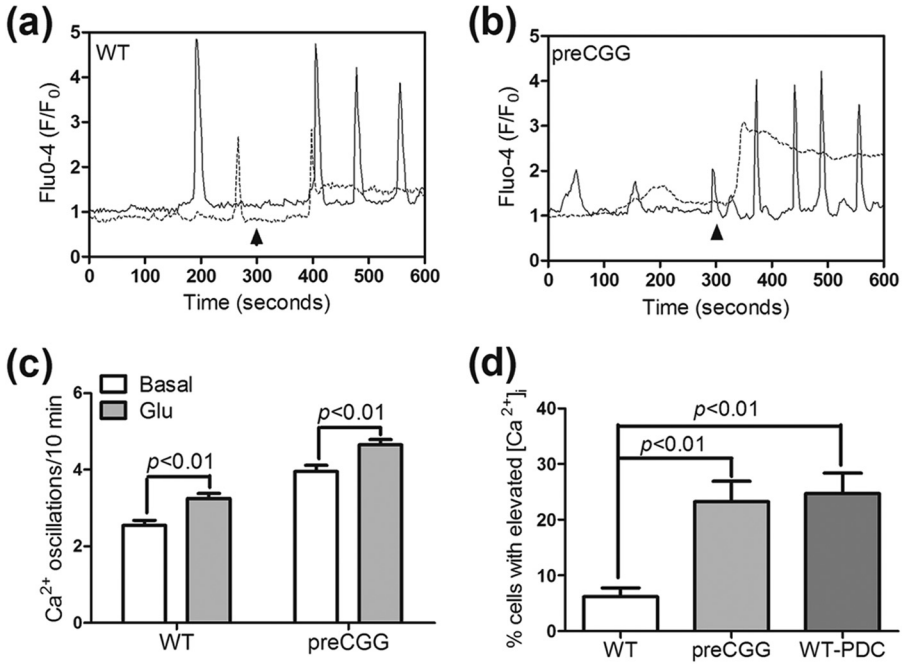

FIGURE 9. **Influence of Glu on the Ca^{2+} dynamics in WT and preCGG cortical astrocytes.** *a* and *b*, representative traces for Glu (10 μM) stimulation of Ca^{2+} response in WT (*a*) and preCGG (*b*) cortical astrocytes. Glu stimulated two distinct Ca^{2+} responses in both WT and preCGG cortical astrocytes. Some cells displayed more Ca^{2+} oscillations (*solid trace*), whereas the remaining responsive cells displayed sustained intracellular Ca^{2+} increase (*dotted trace*). *Arrowheads* indicate the addition of Glu (10 μM). *c*, quantification of the spontaneous Ca^{2+} oscillations before and after 10 μM Glu treatment. A concentration of 10 μM Glu increased the spontaneous Ca^{2+} oscillations in both WT and preCGG astrocytes. Each data point represents the mean ± S.E. from at least 150 cells for each group. *d*, quantification of the percentage of cells with sustained intracellular Ca^{2+} increase after treatment with 10 μM Glu in vehicle or 10 μM L-*trans*-PDC-exposed WT astrocytes and preCGG cortical astrocytes. Each data point represents the mean ± S.E. from at least 4 wells.

ically exposed to 10 μM L-*trans*-PDC for 48 h. Ca^{2+} imaging analysis revealed that a higher percentage (24.7 ± 3.6%, $n = 9$ wells, $p < 0.01$) of L-*trans*-PDC-treated astrocytes displayed sustained intracellular Ca^{2+} increase when compared with the vehicle controls (Fig. 9*d*).

We next evaluated which type of Glu receptors could account for the differences in the Glu-triggered sustained Ca^{2+} response observed between WT and preCGG astrocytes. NMDA, a selective NMDA receptor agonist, had no detectable response on the intracellular Ca^{2+} increase in preCGG cortical astrocytes (Fig. 10*a*). However, the selective mGluR5 antagonist MPEP (10 μM) eliminated the Glu (30 μM)-induced sustained intracellular Ca^{2+} increase in preCGG cortical astrocytes. The mGluR5 agonist, DHPG, at an intermediate concentration of 2 μM, produced a sustained intracellular Ca^{2+} elevation in both WT and preCGG cortical astrocytes. Similar to the response induced by Glu in WT and preCGG astrocytes, a higher percentage of preCGG astrocytes (53.1 ± 4.8%, $n = 4$ wells) displayed sustained intracellular Ca^{2+} increase when compared with WT controls (26.8 ± 6.4%, $n = 4$ wells, $p < 0.01$, Fig. 10*d*). The DHPG-elicited Ca^{2+} response (area under the curve) is also significantly higher in preCGG astrocytes (70.5 ± 9.9, $n = 4$ wells) than in the WT controls (22.4 ± 3.6, $n = 4$ wells, Fig. 10*d*).

PreCGG Cortical Astrocytes Are More Sensitive to Glu Exposure than Are WT Astrocytes—Given the observed differences in Glu-triggered intracellular Ca^{2+} responses between WT and preCGG cortical astrocytes, the concentration-response relationship for Glu was evaluated using FLIPR in a 96-well format. Because individual cells cannot be monitored using FLIPR, it is not possible to detect asynchronous Ca^{2+} oscillations. Nevertheless, this method permits detection of population-averaged Ca^{2+} signals in response to Glu challenge. After recording 3 min of base line, Glu (10–300 μM) or vehicle was introduced into each well simultaneously, and the Ca^{2+} response was recorded for an additional 5 min. Fig. 11 depicts the time- and concentration-response relationships for Glu-induced Ca^{2+} response in both WT and preCGG cortical astrocytes. The EC_{50} values were 35.23 ± 2.80 and 12.94 ± 3.89 μM ($n = 3$, $p < 0.05$) in WT and preCGG cortical astrocytes, respectively. Because FLIPR detects an average cell population response, this measurement likely reflected the increase in both Ca^{2+} oscillations and the sustained rise of intracellular Ca^{2+}. In the *Fmr1* KO mouse model of FXS, excessive protein synthesis downstream of mGluR5 activation following the loss of FMRP expression enhances the long term depression during synaptic transmission (41, 42). In the premutation CGG expansion hippocampal neurons, enhanced neuronal activity which was characterized by clustered burst firing stems, at least in part, from amplified signaling of type I mGluRs (23). Nevertheless, the two genotypes expressed similar levels of mGluR1/5 relative to GFAP (Fig. 12).

DISCUSSION

In this study, we demonstrate that cortical astrocytes isolated from heterozygous KI mice with premutation CGG expansions (~170 repeats) display ~3-fold higher *Fmr1* mRNA levels, yet 30% reduced FMRP expression when compared with paired astrocyte cultures from WT mice. The patterns of these two key markers are consistent with the observations in brain lysates

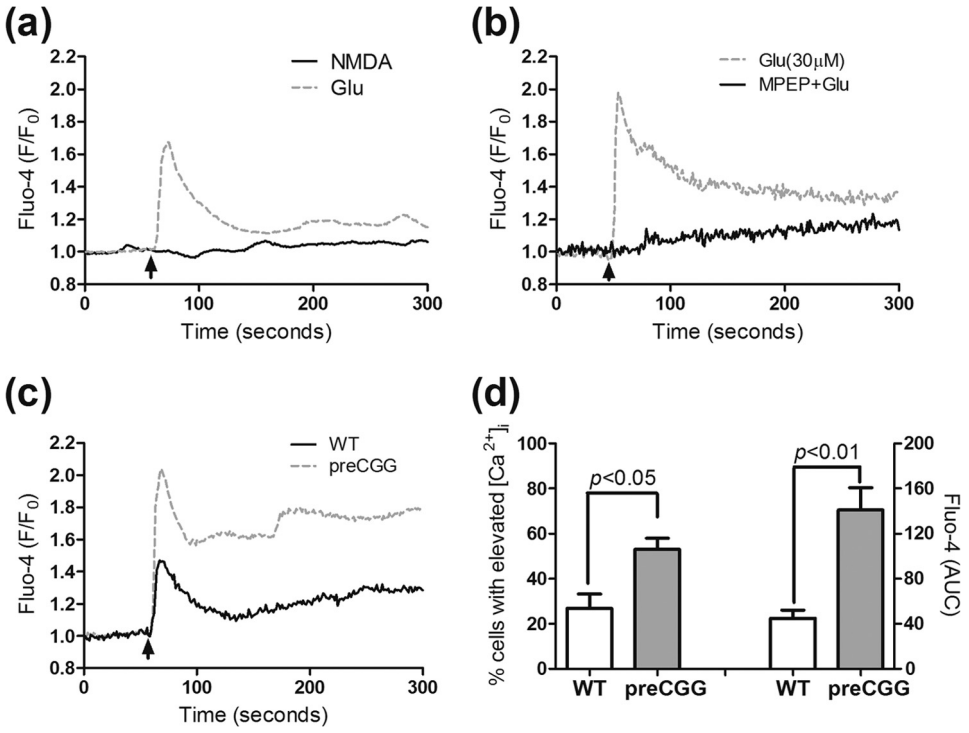

FIGURE 10. **Influence of Glu receptor agonist or antagonist on the Ca^{2+} dynamics in WT or preCGG cortical astrocytes.** *a*, lack of Ca^{2+} response of NMDA in preCGG cortical astrocytes (*solid black line*). Glu (30 μM) was used as a positive control (*gray dotted line*). *b*, An mGluR5 antagonist, MPEP (10 μM) suppressed the Glu (30 μM)-induced intracellular Ca^{2+} increase in preCGG cortical astrocytes. The astrocytes were incubated with MPEP for 10 min before the addition of Glu (*arrowhead*). These data were repeated twice in triplicates with similar results. *c*, representative traces of type I mGluR receptor agonist DHPG (2 μM)-induced intracellular Ca^{2+} increase in both WT and preCGG cortical astrocytes. *Black solid trace*, WT; *gray dotted trace*, preCGG. These data were repeated twice in duplicates with similar results. *d*, quantification of the percentage of cells with sustained intracellular Ca^{2+} increase as well as Ca^{2+} response (area under the curve, *AUC*) after WT and preCGG cortical astrocytes were exposed to 2 μM DHPG. These data were from two independent cultures in duplicates.

from KI mice with preCGG expansions and from postmortem brain from human premutation carriers as well as those with clinical FXTAS (18, 23, 43–45). Neurons cultured from preCGG KI mice also maintain a pattern of elevated *Fmr1* mRNA and modest to moderately reduced FMRP in *vitro* (21, 23). The aberrant Ca^{2+} dynamics, deficits in Glu uptake, and hypersensitivity to Glu receptor signaling reported here, coupled with previous studies of ubiquitin-positive inclusion bodies found in astrocytes in intact brain (15, 32), indicate that histopathological and functional abnormalities extend to preCGG astrocytes.

Cortical astrocytes cultured from preCGG KI mice are shown for the first time to display a higher frequency of asynchronous spontaneous Ca^{2+} oscillations. Alterations in Ca^{2+} dynamics have been demonstrated in neurons cultured from FMRP-null models of FXS (46, 47) as well as *Fmr1* preCGG mouse neuronal cultures (23) and premutation human neurons derived from induced pluripotent stem cells (48). In the null *Fmr1 Drosophila* and *Fmr1* KO mouse models, the Ca^{2+} impairments have been ascribed to the complete loss of FMRP expression. However, recent studies also demonstrated enhanced spontaneous Ca^{2+} oscillations in neurons derived from KI mice and human induced pluripotent stem cells bearing CGG expansion repeats in *FMR1* in the premutation range that maintain >50% of the FMRP expression observed in corresponding WT cells. PreCGG neurons maintain significantly higher (>3-fold) *Fmr1* mRNA levels when compared with neurons derived from their respective WT controls (23, 48), suggesting that an elevated *Fmr1* RNA may also contribute to abnormal growth and Ca^{2+} dynamics observed in neuronal cell models of *Fmr1* related disorders. However, we cannot exclude the potential contribution of reduced levels of FMRP and elevated *Fmr1* mRNA in producing preCGG astrocyte pathophysiology.

Abnormal Ca^{2+} dynamics are associated with modest but consistent decreases in both Glu uptake and expression levels of GLAST and GLT-1 in preCGG astrocyte cultures. Attenuated Glu uptake and Glu transporter expression are likely contributing to the enhanced Ca^{2+} oscillatory behavior observed in preCGG cortical astrocytes because: 1) WT cortical astrocytes chronically exposed to Glu transporter inhibitor pharmacologically display enhanced spontaneous Ca^{2+} oscillations to an extent comparable with that found in preCGG cortical astrocytes; 2) WT astrocytes with reduced GLAST expression (~30%) by siRNA interference exhibit increased spontaneous Ca^{2+} oscillations; and 3) Glu augments Ca^{2+} oscillations in both WT and preCGG cortical astrocyte. The latter is consistent with previous demonstrations for Glu receptor modulating Ca^{2+} oscillations in astrocytes where application of mGluR (group I and group II) antagonists suppressed spontaneous Ca^{2+} oscillations, whereas application of mGluR (group I and group II) agonists evoked Ca^{2+} oscillatory behavior at intermediate concentrations (38). Although how reduced Glu uptake activity influences astrocyte Ca^{2+} signaling remains unclear, reduced Glu uptake activity may transiently affect extracellular

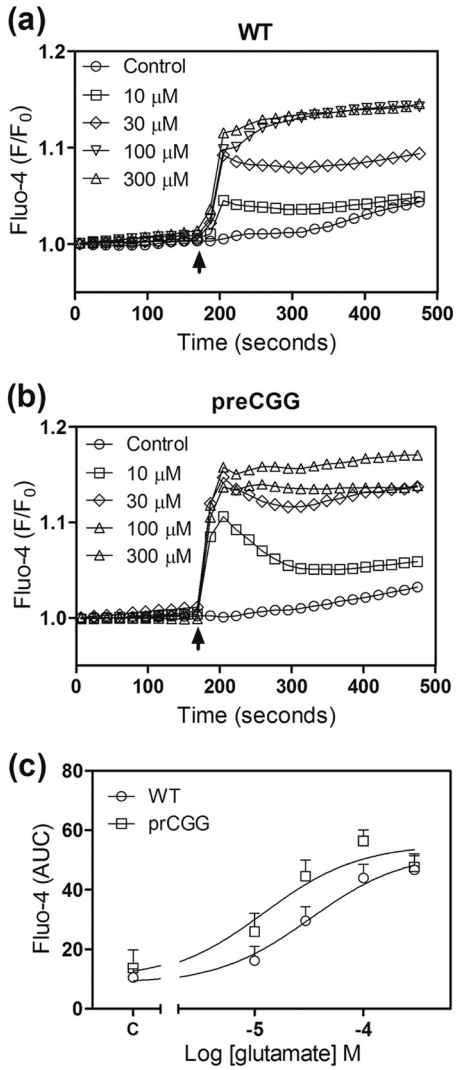

FIGURE 11. **PreCGG cortical astrocytes are more sensitive to Glu exposure measured in a population level.** *a* and *b*, Glu-induced Ca^{2+} response in WT (*a*) and preCGG (*b*) cortical astrocytes (*error bars* are omitted for clarity). *c*, concentration-response relationships for Glu-induced Ca^{2+} response (area under the curve, *AUC*) in WT and preCGG cortical astrocytes. Each data point represents mean ± S.E. ($n = 8$). The experiments were repeated three times, and the EC_{50} values were 35.23 ± 2.80 and 12.94 ± 3.89 μM ($n = 3$, $p < 0.05$) for Glu-induced Ca^{2+} response in WT and preCGG cortical astrocytes, respectively.

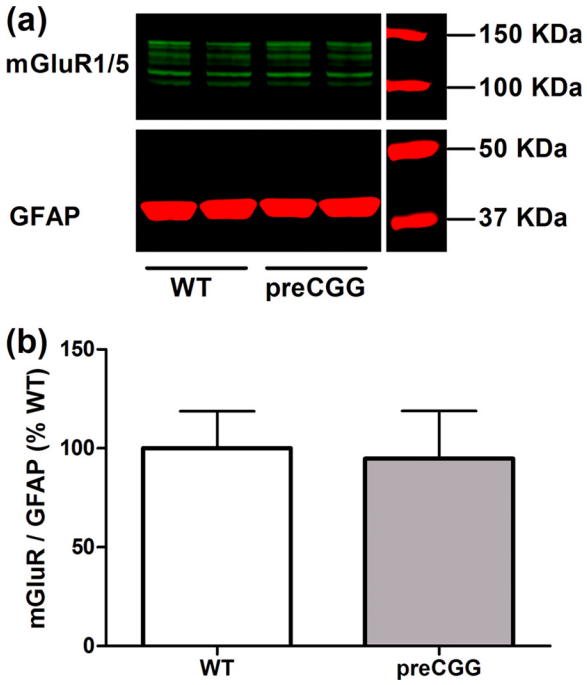

FIGURE 12. **PreCGG cortical astrocytes display similar expression levels of mGluR1/5.** *a*, representative Western blots for mGluR1/5 in WT and preCGG cortical astrocytes. *b*, quantification of mGluR1/5 expression in WT and preCGG cortical astrocyte cultures relative to GFAP. The expression levels for mGluR1/5 were similar to WT controls ($n = 8$ from four independent cultures, $p > 0.05$).

Glu concentration, which in turn can stimulate asynchronous Ca^{2+} oscillations (49).

Consistent with reduced expression of Glu transporters in preCGG astrocyte culture, we also demonstrated that cortical lysates from aged preCGG mice (50 ± 3 weeks) display significantly reduced GLAST expression when compared with age-matched WT mice. GLT-1 expression in preCGG brain cortex was also lower than that found in WT cortex, although the difference was not statistically significant due to the variation in the expression levels. A consistent trend of lower GLAST expression was also observed in younger (~20 weeks) preCGG mice (~155 CGG repeats) brain cortices relative to age-matched WT, but no differences in GLT-1 were detectable at younger ages (P0, P14, P20, and P35; data not shown). Collectively, these data suggest that the deficit in Glu transporters may progress with age in the preCGG KI mouse model.

Impaired Glu uptake has been reported in preCGG hippocampal astrocytes, which have lower affinity for Glu uptake than WT (23). This functional deficit is responsible, at least in part, for the aberrant neuronal network firing, which is likely directly pertinent to the reduced neuronal complexity identified in the same *in vitro* preCGG model (21). Embryonic premutation mice display early migration defects in the neocortex and altered expression of neuronal lineage markers (22). The abnormal asynchronous Ca^{2+} oscillatory behavior observed in preCGG astrocytes reported here offers more direct evidence of an inherent functional impairment that may indirectly contribute to abnormal neuronal cell growth because cellular Ca^{2+} dynamics are known to regulate the release of gliotransmitters, including Glu (50). Moreover, astrocytes can influence neuronal connectivity by improper clearance of Glu from synaptic sites (51). Reduction in Glu uptake can stimulate extrasynaptic NMDA and metabotropic glutamate receptor activation at hippocampal CA1 synapses of aged rats (52). Therefore, impaired Glu uptake as well as a higher frequency of spontaneous Ca^{2+} oscillations observed in preCGG astrocytes may contribute to neuropathological changes observed in premutation models and possibly to the etiology of FXTAS.

Altered Glu transport has been recently reported in *Fmr1* KO astrocytes co-cultured with either WT or *Fmr1* KO neurons (53). However, unlike our present finding in the preCGG KI model, *Fmr1* KO astrocyte cultures showed similar levels of expression of both GLT-1 and GLAST when compared with WT controls. Another distinction between *Fmr1* KO and *FMR1* preCGG KI astrocytes is that the deficits of Glu transporters have been ascribed to reduced mGluR5 expression,

which is regulated by FMRP (53), a difference not observed in the current study of preCGG cortical astrocytes, which maintain a moderate level of FMRP.

PreCGG astrocytes are functionally more sensitive than WT to Glu challenge. This is consistent with similar results obtained from induced pluripotent stem cell neurons derived from a patient with an *FMR1* premutation expansion (48), as well as neuronal/astrocyte co-cultures and slices from preCGG mouse hippocampus that exhibit amplified type I mGluR-dependent clustered burst firing and enhanced mGluR-dependent long term depression, which is positively associated with the CGG repeat length (23, 54, 55).

The influence of abnormal astrocytes on neuronal development has also been demonstrated in other neurological disorders, such as Rett syndrome and FXS (28, 31). Restoration of MeCP2 in the astrocytes possessing mutant Mecp2 allele exerted a non-cell-autonomous positive effect on mutant neurons *in vivo*, restoring dendritic morphology and increasing the excitatory Glu transporter VGLUT1 level (31). Reactive astrocytes have been reported in an FXS mouse model (37). Co-culture with normal astrocytes prevented the development of abnormal dendrite morphology and precluded the reduction of presynaptic and postsynaptic protein clusters in neurons from a fragile X mouse (28). It is conceivable that correction of astrocyte pathology may be a potential therapeutic intervention to ameliorate the neuropathology of FXTAS.

In summary, we demonstrate alternations in Ca^{2+} dynamics and Glu uptake in mouse preCGG cortical astrocytes. It appears that the reduced Glu transporter activity leads to the enhanced spontaneous Ca^{2+} oscillations in preCGG cortical astrocytes. These deficits in astrocytes ultimately may contribute to the development of the neuronal pathology of FXTAS. Thus, the function of the rescue astrocytes may represent a potential therapeutic invention to ameliorate the neuropathology of FXTAS.

Acknowledgments—We thank Binh Ta for carrying out all of the genotyping and Lee Rognlie-Howes for coordinating the breeding of mice used in this study.

REFERENCES

1. Hagerman, P. J. (2008) The fragile X prevalence paradox. *J. Med. Genet.* **45,** 498–499
2. Rodriguez-Revenga, L., Madrigal, I., Pagonabarraga, J., Xunclà, M., Badenas, C., Kulisevsky, J., Gomez, B., and Milà, M. (2009) Penetrance of *FMR1* premutation associated pathologies in fragile X syndrome families. *Eur. J. Hum. Genet.* **17,** 1359–1362
3. Goodlin-Jones, B. L., Tassone, F., Gane, L. W., and Hagerman, R. J. (2004) Autistic spectrum disorder and the fragile X premutation. *J. Dev. Behav. Pediatr.* **25,** 392–398
4. Hessl, D., Tassone, F., Loesch, D. Z., Berry-Kravis, E., Leehey, M. A., Gane, L. W., Barbato, I., Rice, C., Gould, E., Hall, D. A., Grigsby, J., Wegelin, J. A., Harris, S., Lewin, F., Weinberg, D., Hagerman, P. J., and Hagerman, R. J. (2005) Abnormal elevation of *FMR1* mRNA is associated with psychological symptoms in individuals with the fragile X premutation. *Am. J. Med. Genet. B Neuropsychiatr. Genet.* **139B,** 115–121
5. Farzin, F., Perry, H., Hessl, D., Loesch, D., Cohen, J., Bacalman, S., Gane, L., Tassone, F., Hagerman, P., and Hagerman, R. (2006) Autism spectrum disorders and attention-deficit/hyperactivity disorder in boys with the fragile X premutation. *J. Dev. Behav. Pediatr.* **27,** S137–S144
6. Hagerman, R. J. (2006) Lessons from fragile X regarding neurobiology, autism, and neurodegeneration. *J. Dev. Behav. Pediatr.* **27,** 63–74
7. Amiri, K., Hagerman, R. J., and Hagerman, P. J. (2008) Fragile X-associated tremor/ataxia syndrome: an aging face of the fragile X gene. *Arch. Neurol.* **65,** 19–25
8. Brouwer, J. R., Willemsen, R., and Oostra, B. A. (2009) The *FMR1* gene and fragile X-associated tremor/ataxia syndrome. *Am. J. Med. Genet. B Neuropsychiatr. Genet.* **150B,** 782–798
9. Tassone, F., Adams, J., Berry-Kravis, E. M., Cohen, S. S., Brusco, A., Leehey, M. A., Li, L., Hagerman, R. J., and Hagerman, P. J. (2007) CGG repeat length correlates with age of onset of motor signs of the fragile X-associated tremor/ataxia syndrome (FXTAS). *Am. J. Med. Genet. B Neuropsychiatr. Genet.* **144B,** 566–569
10. Berry-Kravis, E., Abrams, L., Coffey, S. M., Hall, D. A., Greco, C., Gane, L. W., Grigsby, J., Bourgeois, J. A., Finucane, B., Jacquemont, S., Brunberg, J. A., Zhang, L., Lin, J., Tassone, F., Hagerman, P. J., Hagerman, R. J., and Leehey, M. A. (2007) Fragile X-associated tremor/ataxia syndrome: clinical features, genetics, and testing guidelines. *Movement Disorders* **22,** 2018–2030
11. Bourgeois, J. A., Coffey, S. M., Rivera, S. M., Hessl, D., Gane, L. W., Tassone, F., Greco, C., Finucane, B., Nelson, L., Berry-Kravis, E., Grigsby, J., Hagerman, P. J., and Hagerman, R. J. (2009) A review of fragile X premutation disorders: expanding the psychiatric perspective. *J. Clin. Psychiatry* **70,** 852–862
12. Jacquemont, S., Hagerman, R. J., Hagerman, P. J., and Leehey, M. A. (2007) Fragile-X syndrome and fragile X-associated tremor/ataxia syndrome: two faces of FMR1. *Lancet Neurol.* **6,** 45–55
13. Hagerman, R., Au, J., and Hagerman, P. (2011) *FMR1* premutation and full mutation molecular mechanisms related to autism. *J. Neurodev. Disord.* **3,** 211–224
14. Tassone, F., Hagerman, R. J., Taylor, A. K., Gane, L. W., Godfrey, T. E., and Hagerman, P. J. (2000) Elevated levels of *FMR1* mRNA in carrier males: a new mechanism of involvement in the fragile-X syndrome. *Am. J. Hum. Genet.* **66,** 6–15
15. Willemsen, R., Hoogeveen-Westerveld, M., Reis, S., Holstege, J., Severijnen, L. A., Nieuwenhuizen, I. M., Schrier, M., van Unen, L., Tassone, F., Hoogeveen, A. T., Hagerman, P. J., Mientjes, E. J., and Oostra, B. A. (2003) The FMR1 CGG repeat mouse displays ubiquitin-positive intranuclear neuronal inclusions; implications for the cerebellar tremor/ataxia syndrome. *Hum. Mol. Genet.* **12,** 949–959
16. Brouwer, J. R., Mientjes, E. J., Bakker, C. E., Nieuwenhuizen, I. M., Severijnen, L. A., Van der Linde, H. C., Nelson, D. L., Oostra, B. A., and Willemsen, R. (2007) Elevated *Fmr1* mRNA levels and reduced protein expression in a mouse model with an unmethylated Fragile X full mutation. *Exp. Cell Res.* **313,** 244–253
17. Jacquemont, S., Farzin, F., Hall, D., Leehey, M., Tassone, F., Gane, L., Zhang, L., Grigsby, J., Jardini, T., Lewin, F., Berry-Kravis, E., Hagerman, P. J., and Hagerman, R. J. (2004) Aging in individuals with the *FMR1* mutation. *Am. J. Ment. Retard.* **109,** 154–164
18. Tassone, F., Iwahashi, C., and Hagerman, P. J. (2004) FMR1 RNA within the intranuclear inclusions of fragile X-associated tremor/ataxia syndrome (FXTAS). *RNA Biol.* **1,** 103–105
19. Greco, C. M., Hagerman, R. J., Tassone, F., Chudley, A. E., Del Bigio, M. R., Jacquemont, S., Leehey, M., and Hagerman, P. J. (2002) Neuronal intranuclear inclusions in a new cerebellar tremor/ataxia syndrome among fragile X carriers. *Brain* **125,** 1760–1771
20. Arocena, D. G., Iwahashi, C. K., Won, N., Beilina, A., Ludwig, A. L., Tassone, F., Schwartz, P. H., and Hagerman, P. J. (2005) Induction of inclusion formation and disruption of lamin A/C structure by premutation CGG-repeat RNA in human cultured neural cells. *Hum. Mol. Genet.* **14,** 3661–3671
21. Chen, Y., Tassone, F., Berman, R. F., Hagerman, P. J., Hagerman, R. J., Willemsen, R., and Pessah, I. N. (2010) Murine hippocampal neurons expressing *Fmr1* gene premutations show early developmental deficits and late degeneration. *Hum. Mol. Genet.* **19,** 196–208
22. Cunningham, C. L., Martínez Cerdeño, V., Navarro Porras, E., Prakash, A. N., Angelastro, J. M., Willemsen, R., Hagerman, P. J., Pessah, I. N., Berman, R. F., and Noctor, S. C. (2011) Premutation CGG-repeat expan-

sion of the *Fmr1* gene impairs mouse neocortical development. *Hum. Mol. Genet.* **20,** 64–79
23. Cao, Z., Hulsizer, S., Tassone, F., Tang, H. T., Hagerman, R. J., Rogawski, M. A., Hagerman, P. J., and Pessah, I. N. (2012) Clustered burst firing in *FMR1* premutation hippocampal neurons: amelioration with allopregnanolone. *Hum. Mol. Genet.* **21,** 2923–2935
24. Kaplan, E. S., Cao, Z., Hulsizer, S., Tassone, F., Berman, R. F., Hagerman, P. J., and Pessah, I. N. (2012) Early mitochondrial abnormalities in hippocampal neurons cultured from *Fmr1* pre-mutation mouse model. *J. Neurochem.* **123,** 613–621
25. Haydon, P. G. (2001) GLIA: listening and talking to the synapse. *Nat. Rev. Neurosci.* **2,** 185–193
26. Ben Achour, S., Pont-Lezica, L., Béchade, C., and Pascual, O. (2010) Is astrocyte calcium signaling relevant for synaptic plasticity? *Neuron Glia Biol.* **6,** 147–155
27. Jacobs, S., Nathwani, M., and Doering, L. C. (2010) Fragile X astrocytes induce developmental delays in dendrite maturation and synaptic protein expression. *BMC Neurosci.* **11,** 132
28. Jacobs, S., and Doering, L. C. (2010) Astrocytes prevent abnormal neuronal development in the fragile X mouse. *J. Neurosci.* **30,** 4508–4514
29. Maezawa, I., Swanberg, S., Harvey, D., LaSalle, J. M., and Jin, L. W. (2009) Rett syndrome astrocytes are abnormal and spread MeCP2 deficiency through gap junctions. *J. Neurosci.* **29,** 5051–5061
30. Maezawa, I., and Jin, L. W. (2010) Rett syndrome microglia damage dendrites and synapses by the elevated release of glutamate. *J. Neurosci.* **30,** 5346–5356
31. Lioy, D. T., Garg, S. K., Monaghan, C. E., Raber, J., Foust, K. D., Kaspar, B. K., Hirrlinger, P. G., Kirchhoff, F., Bissonnette, J. M., Ballas, N., and Mandel, G. (2011) A role for glia in the progression of Rett's syndrome. *Nature* **475,** 497–500
32. Wenzel, H. J., Hunsaker, M. R., Greco, C. M., Willemsen, R., and Berman, R. F. (2010) Ubiquitin-positive intranuclear inclusions in neuronal and glial cells in a mouse model of the fragile X premutation. *Brain Res.* **1318,** 155–166
33. Greco, C. M., Berman, R. F., Martin, R. M., Tassone, F., Schwartz, P. H., Chang, A., Trapp, B. D., Iwahashi, C., Brunberg, J., Grigsby, J., Hessl, D., Becker, E. J., Papazian, J., Leehey, M. A., Hagerman, R. J., and Hagerman, P. J. (2006) Neuropathology of fragile X-associated tremor/ataxia syndrome (FXTAS). *Brain* **129,** 243–255
34. Iwahashi, C., Tassone, F., Hagerman, R. J., Yasui, D., Parrott, G., Nguyen, D., Mayeur, G., and Hagerman, P. J. (2009) A quantitative ELISA assay for the fragile X mental retardation 1 protein. *J. Mol. Diagn.* **11,** 281–289
35. Cao, Z., LePage, K. T., Frederick, M. O., Nicolaou, K. C., and Murray, T. F. (2010) Involvement of caspase activation in azaspiracid-induced neurotoxicity in neocortical neurons. *Toxicol. Sci.* **114,** 323–334
36. Cao, Z., Hammock, B. D., McCoy, M., Rogawski, M. A., Lein, P. J., and Pessah, I. N. (2012) Tetramethylenedisulfotetramine alters Ca^{2+} dynamics in cultured hippocampal neurons: mitigation by NMDA receptor blockade and $GABA_A$ receptor-positive modulation. *Toxicol. Sci.* **130,** 362–372
37. Yuskaitis, C. J., Beurel, E., and Jope, R. S. (2010) Evidence of reactive astrocytes but not peripheral immune system activation in a mouse model of Fragile X syndrome. *Biochim. Biophys. Acta* **1802,** 1006–1012
38. Zur Nieden, R., and Deitmer, J. W. (2006) The role of metabotropic glutamate receptors for the generation of calcium oscillations in rat hippocampal astrocytes *in situ*. *Cereb. Cortex.* **16,** 676–687
39. Rothstein, J. D., Dykes-Hoberg, M., Pardo, C. A., Bristol, L. A., Jin, L., Kuncl, R. W., Kanai, Y., Hediger, M. A., Wang, Y., Schielke, J. P., and Welty, D. F. (1996) Knockout of glutamate transporters reveals a major role for astroglial transport in excitotoxicity and clearance of glutamate. *Neuron* **16,** 675–686
40. Arriza, J. L., Fairman, W. A., Wadiche, J. I., Murdoch, G. H., Kavanaugh, M. P., and Amara, S. G. (1994) Functional comparisons of three glutamate transporter subtypes cloned from human motor cortex. *J. Neurosci.* **14,** 5559–5569
41. Huber, K. M., Gallagher, S. M., Warren, S. T., and Bear, M. F. (2002) Altered synaptic plasticity in a mouse model of fragile X mental retardation. *Proc. Natl. Acad. Sci. U.S.A.* **99,** 7746–7750
42. Bear, M. F., Huber, K. M., and Warren, S. T. (2004) The mGluR theory of fragile X mental retardation. *Trends Neurosci.* **27,** 370–377
43. Brouwer, J. R., Severijnen, E., de Jong, F. H., Hessl, D., Hagerman, R. J., Oostra, B. A., and Willemsen, R. (2008) Altered hypothalamus-pituitary-adrenal gland axis regulation in the expanded CGG-repeat mouse model for fragile X-associated tremor/ataxia syndrome. *Psychoneuroendocrinology* **33,** 863–873
44. Brouwer, J. R., Huizer, K., Severijnen, L. A., Hukema, R. K., Berman, R. F., Oostra, B. A., and Willemsen, R. (2008) CGG-repeat length and neuropathological and molecular correlates in a mouse model for fragile X-associated tremor/ataxia syndrome. *J. Neurochem.* **107,** 1671–1682
45. Allen, E. G., He, W., Yadav-Shah, M., and Sherman, S. L. (2004) A study of the distributional characteristics of FMR1 transcript levels in 238 individuals. *Hum. Genet.* **114,** 439–447
46. Tessier, C. R., and Broadie, K. (2011) The fragile X mental retardation protein developmentally regulates the strength and fidelity of calcium signaling in Drosophila mushroom body neurons. *Neurobiol. Dis.* **41,** 147–159
47. Deng, P. Y., Sojka, D., and Klyachko, V. A. (2011) Abnormal presynaptic short-term plasticity and information processing in a mouse model of fragile X syndrome. *J. Neurosci.* **31,** 10971–10982
48. Liu, J., Koscielska, K. A., Cao, Z., Hulsizer, S., Grace, N., Mitchell, G., Nacey, C., Githinji, J., McGee, J., Garcia-Arocena, D., Hagerman, R. J., Nolta, J., Pessah, I. N., and Hagerman, P. J. (2012) Signaling defects in iPSC-derived fragile X premutation neurons. *Hum. Mol. Genet.* **21,** 3795–3805
49. Padmashri, R., and Sikdar, S. K. (2008) Glutamate transporter blockade affects Ca^{2+} responses in astrocytes. *Neuroscience* **151,** 56–62
50. Koizumi, S., Fujishita, K., Tsuda, M., Shigemoto-Mogami, Y., and Inoue, K. (2003) Dynamic inhibition of excitatory synaptic transmission by astrocyte-derived ATP in hippocampal cultures. *Proc. Natl. Acad. Sci. U.S.A.* **100,** 11023–11028
51. Oliet, S. H., Piet, R., and Poulain, D. A. (2001) Control of glutamate clearance and synaptic efficacy by glial coverage of neurons. *Science* **292,** 923–926
52. Potier, B., Billard, J. M., Rivière, S., Sinet, P. M., Denis, I., Champeil-Potokar, G., Grintal, B., Jouvenceau, A., Kollen, M., and Dutar, P. (2010) Reduction in glutamate uptake is associated with extrasynaptic NMDA and metabotropic glutamate receptor activation at the hippocampal CA1 synapse of aged rats. *Aging Cell* **9,** 722–735
53. Higashimori, H., Morel, L., Huth, J., Lindemann, L., Dulla, C., Taylor, A., Freeman, M., and Yang, Y. (2013) Astroglial FMRP-dependent translational down-regulation of mGluR5 underlies glutamate transporter GLT1 dysregulation in the fragile X mouse. *Hum Mol Genet.*, in press
54. Iliff, A. J., Renoux, A. J., Krans, A., Usdin, K., Sutton, M. A., and Todd, P. K. (2013) Impaired activity-dependent FMRP translation and enhanced mGluR-dependent LTD in Fragile X premutation mice. *Hum. Mol. Genet.* **22,** 1180–1192
55. Hunsaker, M. R., Kim, K., Willemsen, R., and Berman, R. F. (2012) CGG trinucleotide repeat length modulates neural plasticity and spatiotemporal processing in a mouse model of the fragile X premutation. *Hippocampus* **22,** 2260–2275